Electronic Supplementary Information

X-shaped benzoylbenzophenone derivatives with crossed donors and acceptors for highly efficient thermally activated delayed fluorescence

Sae Youn Lee,[a] Takuma Yasuda,[a,b,c]* In Seob Park [a] and Chihaya Adachi[a,b]*

[a]*Department of Applied Chemistry and Center for Organic Photonics and Electronics Research (OPERA), Kyushu University, 744 Motooka, Nishi, Fukuoka 819-0395 Japan E-mail: yasuda@ifrc.kyushu-u.ac.jp, adachi@cstf.kyushu-u.ac.jp*
[b]*International Institute for Carbon Neutral Energy Research (WPI-I2CNER), Kyushu University, 744 Motooka, Nishi, Fukuoka 819-0395, Japan*
[c]*INAMORI Frontier Research Center, Kyushu University, 744 Motooka, Nishi, Fukuoka 819-0395, Japan*

General.

NMR spectra were recorded on an Avance III 500 spectrometer (Bruker). Chemical shifts of ^{1}H NMR signals were quoted to tetramethylsilane (δ = 0.00) as an internal standards. Matrix-assisted laser desorption ionization time-of-flight (MALDI-TOF) mass spectra were collected on a Autoflex III spectrometer (Bruker Daltonics) using dithranol as the matrix. Elemental analyses were carried out with a Yanaco MT-5 CHN corder. The UV/vis absorption and PL spectra of organic films were measured with a UV-2550 (Shimadzu) and a FluoroMax-4 spectrofluorometer (Horiba Scientific), respectively. The photoluminescence quantum efficiency (Φ_{PL}) was measured using an absolute PL quantum yield measurement system (Hamamatsu Photonics C9920-02, PMA-11). Luminescence intensity and lifetime of organic films were measured with a Streak camera (Hamamatsu Photonics C4334). The organic films were excited by an N_2 gas laser (λ = 337 nm, pulse width = 500 ps, repetition rate 20 Hz) under a vacuum of < 4×10^{-1} Pa. Samples were cooled down at 5 K with a cryostat (Iwatani Industrial Gases). The density-functional theory (DFT) computations were performed on the Gaussian 03 program package,[S1] using the B3LYP functional with the 6-31G(d,p) basis set.

Materials and syntheses.

All reagent and solvent were purchased from Sigma-Aldrich, Tokyo Chemical Industry (TCI), or Wako Pure Chemical Industries and used as received unless otherwise noted. The synthetic route to obtain **AcPmBPX** and **PxPmBPX** are outlined in Scheme S1. All reactions were performed under an N_2 atmosphere in dry solvents.

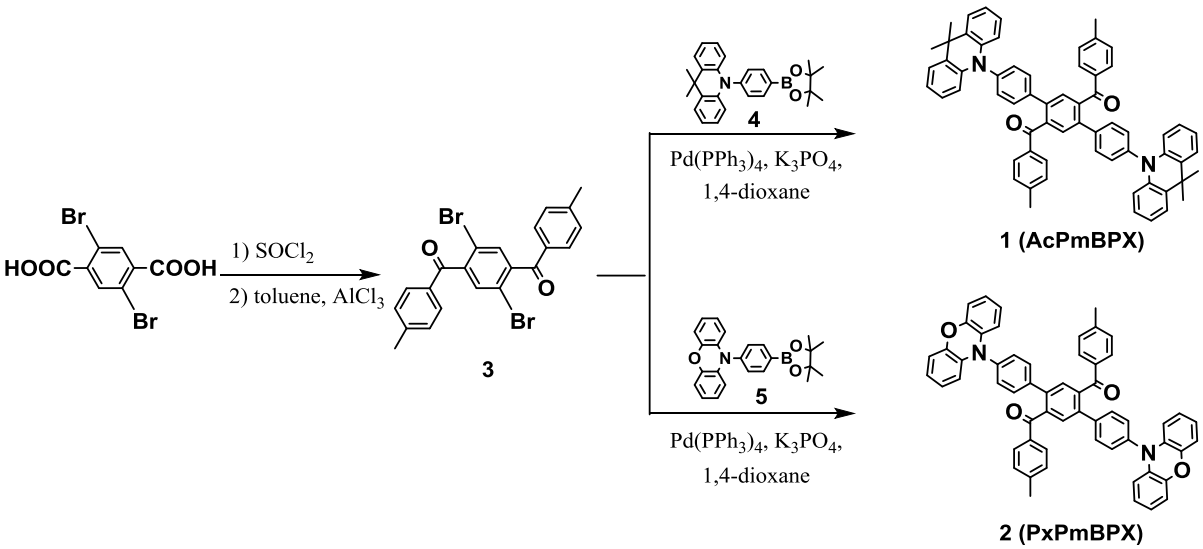

Scheme S1 Synthetic route for **AcPmBPX** and **PxPmBPX**.

1,4-Dibromo-2,5-bis(*p*-tolyl-methanoyl)benzene (3) A mixture of 2,5-diboromoterephtalic acid (6.48 g, 0.02 mol) and thionyl chloride (4.1 mL) was refluxed for 3 h. The excess thionyl chloride was removed under vacuum to give 2,5-dibromoterephtalic acid chloride as a yellow crystalline solid. To a solution of 2,5-dibromoterephtalic acid chloride in toluene (40 mL), aluminum trichloride (5.60 g, 0.04 mol) was added slowly at 0 ℃. The mixture was allowed to react for 1 h at that temperature. Then, the mixture was heated at 90 ℃ for 1 h, cooled down to 40 ℃, and reacted overnight. Upon cooling to room temperature, the reaction mixture was poured into water to precipitate a white solid which was isolated by filtration. The crude product was recrystallized from chloroform and methanol to give a white solid (yield = 7.11 g, 75.3%). ^{1}H NMR (500 MHz, $CDCl_3$): δ 7.75 (d, J = 8.0Hz, 4H), 7.58 (s, 2H), 7.32 (d, J = 8.0 Hz, 4H), 7.32 (d, J = 7.5 Hz, 4H), 2.46 (s, 6H). MS (MALDI): *m/z* 472.32 $[M+H]^+$; calcd 472.17.

1,4-Bis(9,9-dimethylacridan-10-yl-*p*-phenyl)-2,5-bis(*p*-tolyl-methanoyl)benzene (1, AcPmBPX) Compounds **3** (0.94 g, 2.0 mmol) and **4** (1.81 g, 4.4 mmol) were dissolved in 1,4-dioxane (40 mL) under N_2 atmosphere. To the solution were added aqueous potassium phosphate (2 M, 10 mL) and tertrakis(triphenylphosphine)palladium(0) (0.14 g, 0.12 mmol). After the complete addition, the mixture was refluxed for 48 h. The reaction mixture was then poured into water. The product was extracted with dichloromethane. The combined organic layers were washed with water and dried over anhydrous $MgSO_4$. After filtration and evaporation, the crude material was purified by column chromatography on silica gel (eluent: dichloromethane/hexane, 1:1 v/v) and dried under vacuum to give a white powder (yield = 1.27 g, 72.1%). This compound was further purified by temperature-gradient sublimation under vacuum. ^{1}H NMR (500 MHz, $CDCl_3$): δ 7.87 (s, 2H), 7.63 (t, J = 7.0 Hz, 8H), 7.43 (d, J = 7.0 Hz, 4H), 7.19-7.16 (m, 8H), 6.91-6.88 (m, 8H), 5.86 (d, J = 7.5 Hz, 4H), 2.41 (s, 6H), 1.65 (s, 12H). MS (MALDI): *m/z* 882.12 $[M]^+$; calcd 882.12. Anal. calcd (%) for $C_{64}H_{52}N_2O_2$: C, 87.24; H, 5.95; N, 3.18; found: C, 87.19; H, 5.87; N, 3.24.

1,4-Bis(9,9-phenoxazin-10-yl-*p*-phenyl)-2,5-bis(*p*-tolyl-methanoyl)benzene (2, PxPmBPX) This compound was synthesized using a procedure similar to that employed for the synthesis of **1** except that **5** was used instead of **4** (yield = 1.34 g, 80.7%). This compound was further purified by temperature-gradient sublimation under vacuum. ^{1}H NMR (500 MHz, $CDCl_3$): δ 7.81 (s, 2H), 7.61-7.56 (m, 8H), 7.18 (d, J = 8.0 Hz, 4H), 7.14 (d, J = 8.0 Hz, 4H), 6.67-6.61 (m, 8H), 6.53 (td, J = 8.0 Hz, 2.0 Hz, 4H), 5.53 (dd, J = 8.0 Hz, 1.0 Hz, 4H), 2.37 (s, 6H). MS (MALDI): *m/z* 828.94 $[M]^+$; calcd 828.95. Anal. calcd (%) for $C_{58}H_{40}N_2O_4$: C, 84.04; H, 4.86; N, 3.38; found: C, 83.98; H, 4.96; N, 3.45.

Determination of radiative decay, ISC, and RISC rate constants.

In the presence of intersystem crossing (ISC) and reverse intersystem crossing (RISC) between the S_1 and T_1 states, the rate constants of the prompt and delayed PL components (k_p and k_d, respectively) can be expressed as follows:[S2]

$$k_p = \frac{1}{\tau_p} = k_r^S + k_{nr}^S + k_{ISC} \qquad (1)$$

$$k_{\mathrm{d}} = \frac{1}{\tau_{\mathrm{d}}} = k_{\mathrm{nr}}^{\mathrm{T}} + \left(1 - \frac{k_{\mathrm{ISC}}}{k_{\mathrm{r}}^{\mathrm{S}} + k_{\mathrm{nr}}^{\mathrm{S}} + k_{\mathrm{ISC}}}\right) k_{\mathrm{RISC}} \qquad (2)$$

where k_r^S and k_{nr}^S are the radiative and non-radiative decay rate constants of the S_1 state, respectively, and k_{ISC} and k_{RISC} are the ISC ($S_1 \rightarrow T_1$) and RISC ($T_1 \rightarrow S_1$) rate constants, respectively. The rates k_r^S and k_{ISC} are assumed to be much faster than k_{nr}^T and k_{RISC}, which is supported by the much longer decay time of the delayed emission component in the transient PL data.

The PL quantum efficiencies of the prompt and delayed fluorescence components (Φ_F and Φ_{TADF}, respectively) and ISC (Φ_{ISC}) are given by the following equations.

$$\Phi_{\mathrm{F}} = \frac{k_{\mathrm{r}}^{\mathrm{S}}}{k_{\mathrm{r}}^{\mathrm{S}} + k_{\mathrm{nr}}^{\mathrm{S}} + k_{\mathrm{ISC}}} \qquad (3)$$

$$\Phi_{\mathrm{TADF}} = \sum_{k=1}^{\infty} (\Phi_{\mathrm{ISC}}\, \Phi_{\mathrm{RISC}})^k\, \Phi_{\mathrm{F}} \qquad (4)$$

$$\Phi_{\mathrm{ISC}} = \frac{k_{\mathrm{ISC}}}{k_{\mathrm{r}}^{\mathrm{S}} + k_{\mathrm{nr}}^{\mathrm{S}} + k_{\mathrm{ISC}}} \qquad (5)$$

From Eqs. 1 to 5, the following equation can be obtained.

$$k_{\mathrm{RISC}} = \frac{k_{\mathrm{p}} k_{\mathrm{d}}}{k_{\mathrm{ISC}}} \frac{\Phi_{\mathrm{TADF}}}{\Phi_{\mathrm{F}}} \qquad (6)$$

Since the transient PL prompt component exhibits almost negligible temperature dependence at 5–300 K, we can assume that $k_{\mathrm{nr}}^{\mathrm{S}} \approx 0$ at ambient temperature. Based on Eqs. 1 to 6, $k_{\mathrm{r}}^{\mathrm{S}}$, k_{ISC}, and k_{RISC} of **1** and **2** in the doped films can be estimated.

OLED fabrication and measurements.

To measure EL properties, clean glass substrates precoated with a 110-nm-thick indium-tin-oxide (ITO) layer with a sheet resistance of < 20 Ω/□ were used. The substrates was degreased with distilled water, a neutral detergent, acetone, and isopropyl alcohol and then cleaned in UV-ozone chamber (Nippon Laser and Electrics Lab NLUV253) before being loaded into an evaporation system. The organic layers were thermally evaporated on the substrates under a vacuum of < 3×10^{-4} Pa with an evaporation rate of < 0.3 nm/s. In all devices, a cathode aluminum (Al) layer was deposited through a 1 mm-diameter opening in a shadow mask. The current density and voltage (*J*−*V*) characteristics of OLEDs were measured using a semiconductor parameter analyzer (Agilent E5273A). The EL spectra were recorded by a multi channel analyzer (Ocean Optics SD2000) at current densities of 1, 10, and 100 mA/cm^2. The brightness of the OLEDs was measured using an optical powermeter (Newport 1930C).

Table S1 Photophysical properties of **1** and **2.**

Compound	λ_{abs} (nm) sol[a]	λ_{PL} (nm) sol[a] / film[b]	Φ_{PL} (%) sol[a] / film[b]	HOMO (eV)[c]	LUMO (eV)[d]	E_{S} / E_{T} (eV)[e]	ΔE_{ST} (eV)[f]	calc. ΔE_{ST} (eV)[g]
1	281	496/492	20 / 46	−5.80	−2.90	2.79 / 2.74	0.05	0.01
2	282, 318	510/530	10 / 57	−5.60	−2.80	2.70 / 2.72	0.02	0.01

[a] Measured in oxygen-free toluene solution at room temperature. [b] Measured with 6 wt %-doped films in a host matrix (host = mCBP for **1** and **2**). [c] Determined by photoelectron yield spectroscopy in thin films. [d] Deduced from the HOMO and optical energy gap (E_{g}). [e] Singlet (E_{S}) and triplet (E_{T}) energies estimated from onset wavelengths of the doped film emission spectra at 300 and 5 K, respectively. [f] $\Delta E_{\mathrm{ST}} = E_{\mathrm{S}} - E_{\mathrm{T}}$. [g] Calculated by TD-DFT at B3LYP/6-31G(d,p).

Table S2 Rate constants and quantum efficiencies for decay processes in **1** and **2**.[a, S2]

Compound	τ_{p} (ns)	τ_{d} (μs)	$k_{\mathrm{r}}^{\mathrm{S}}$ (s^{-1})	k_{ISC} (s^{-1})	k_{RISC} (s^{-1})	Φ_{F} (%)	Φ_{TADF} (%)	Φ_{ISC} (%)	Φ_{RISC} (%)
1	20	925	1.3×10^{7}	3.7×10^{7}	1.1×10^{3}	26	20	74	27
2	30	314	7.0×10^{6}	2.6×10^{7}	7.0×10^{3}	21	36	79	46

[a] Measured with 6 wt %-doped films in a host matrix (host = mCBP for **1** and **2**).

Table S3 EL performance of TADF-OLEDs based on **1** and **2** as emitter.

Emitter	Host	λ_{EL} (nm)	V_{on} (V)	L_{max} (cd m^{-2})	η_c (cd A^{-1})	η_{ext} (%)
1	mCBP	504	5.2	43749	23.4	10.0
2	mCBP	541	3.2	61040	35.3	11.3

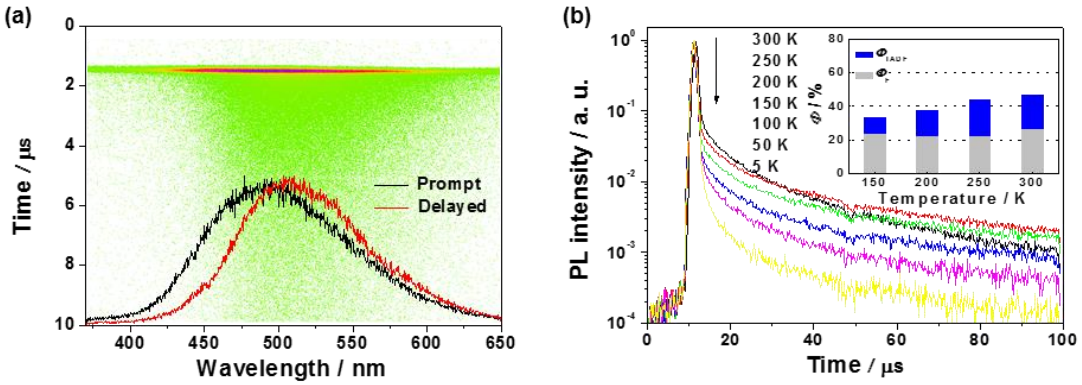

Fig. S1 (a) Streak image and photoluminescence spectra of a 6 wt % **1**:mCBP film showing the prompt (fluorescence, black) and delayed (TADF, red) components. (b) Temperature dependence of transient PL decay from 300 to 5 K. The inset shows the contribution of fluorescence and TADF to the total PL quantum efficiency (Φ_{PL}).

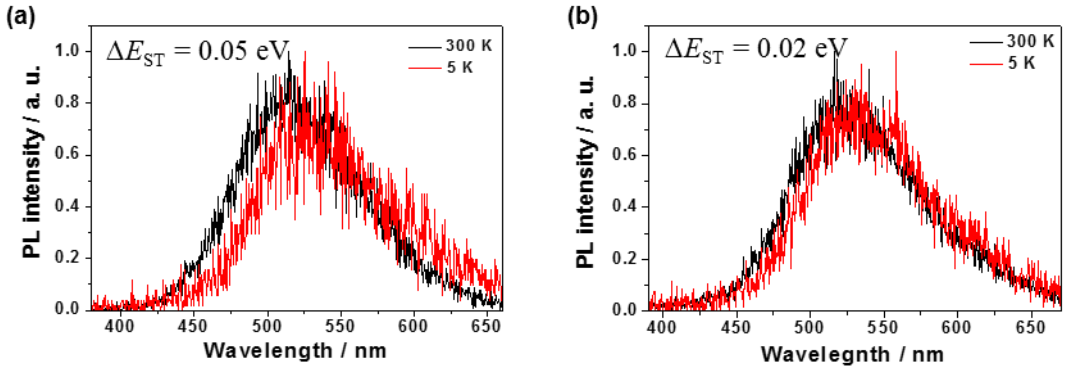

Fig. S2 PL spectra of prompt fluorescence at 300 K (black) and phosphorescence at 5 K (red) for **1** (a) and **2** (b) in 6 wt %-doped films in a host matrix (host = mCBP for **1** and **2**). The TADF intensity is almost negligible at 5 K. ΔE_{ST} was determined from the energy difference between the high-energy onset positions of the fluorescence and phosphorescence spectra.

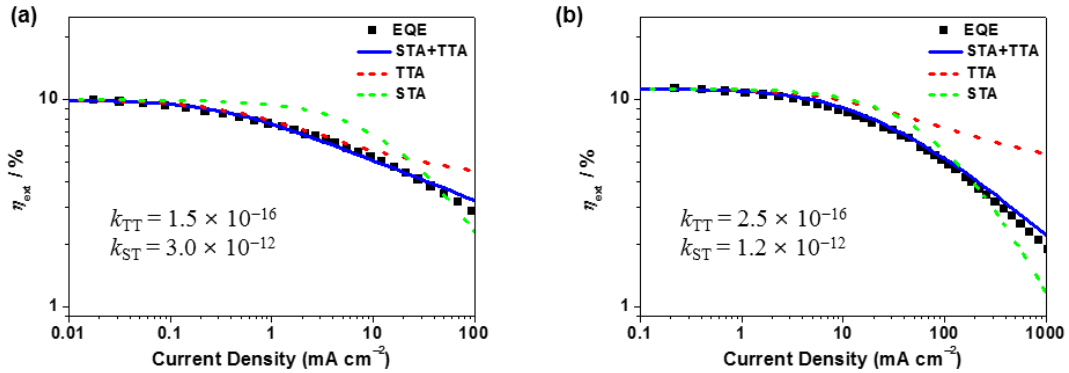

Fig. S3 EL external quantum efficiency (η_{ext}) vs. current density plots of **1**-based (a) and **2**-based (b) device including TTA, STA, and STA and TTA combined process with k_{TT} = 1.5 and 2.5 × 10^{-16} cm^3 s^{-1} and k_{ST} = 3.0 and 1.2 × 10^{-12} cm^3 s^{-1}.[S3]

References

1 M. J. Frisch, G. W. Trucks, H. B. Schlegel, G. E. Scuseria, M. A. Robb, J. R. Cheeseman, J. A. Montgomery, Jr., T. Vreven, K. N. Kudin, J. C. Burant, J. M. Millam, S. S. Iyengar, J. Tomasi, V. Barone, B. Mennucci, M. Cossi, G. Scalmani, N. Rega, G. A. Petersson, H. Nakatsuji, M. Hada, M. Ehara, K. Toyota, R. Fukuda, J. Hasegawa, M. Ishida, T. Nakajima, Y. Honda, O. Kitao, H. Nakai, M. Klene, X. Li, J. E. Knox, H. P. Hratchian, J. B. Cross, C. Adamo, J. Jaramillo, R. Gomperts, R. E. Stratmann, O. Yazyev, A. J. Austin, R. Cammi, C. Pomelli, J. W. Ochterski, P. Y. Ayala, K. Morokuma, G. A. Voth, P. Salvador, J. J. Dannenberg, V. G. Zakrzewski, S. Dapprich, A. D. Daniels, M. C. Strain, O. Farkas, D. K. Malick, A. D. Rabuck, K. Raghavachari, J. B. Foresman, J. V. Ortiz, Q. Cui, A. G. Baboul, S. Clifford, J. Cioslowski, B. B. Stefanov, G. Liu, A. Liashenko, P. Piskorz, I. Komaromi, R. L. Martin, D. J. Fox, T. Keith, M. A. Al-Laham, C. Y. Peng, A. Nanayakkara, M. Challacombe, P. M. W. Gill, B. Johnson, W. Chen, M. W. Wong, C. Gonzalez, J. A. Pople, Gaussian 03, Gaussian, Inc., Pittsburgh PA, **2003**.

2 K. Goushi, K. Yoshida, K. Sato and C. Adachi, *Nat. Photon*., 2012, **6**, 253.

3 K. Masui, H. Nakanotani and C. Adachi, *Org. Electron*., 2013, **14**, 2721.